Relative quantification of deuterated omega-3 and -6 fatty acids and their lipid turnover in PC12 cell membranes using TOF-SIMS

N.B. When citing this work, cite the original published paper.

(article starts on next page)

Relative quantification of deuterated omega-3 and -6 fatty acids and their lipid turnover in PC12 cell membranes using TOF-SIMS[S]

Mai H. Philipsen,*,† **Sanna Sämfors,***,† **Per Malmberg,***,† **and Andrew G. Ewing**[1],*,†,§

Department of Chemistry and Chemical Engineering,* and Go:IMS,† Chalmers University of Technology, and Department of Chemistry and Molecular Biology,§ University of Gothenburg, Gothenburg 412 96, Sweden

ORCID IDs: 0000-0002-7927-0470 (S.S.); 0000-0002-6487-7851 (P.M.); 0000-0002-2084-0133 (A.G.E.)

Abstract Understanding FA metabolism and lipid synthesis requires a lot of information about which FAs and lipids are formed within the cells. We focused on the use of deuterated substrates of 100 µM α-linolenic acid and linoleic acid to determine the relative amounts of their converted PUFAs and specific phospholipids that are incorporated into cell plasma membranes. Time-of-flight secondary ion mass spectrometry (TOF-SIMS) was used to image and analyze lipids in model cell membranes with and without FA treatment. Because of its high spatial resolution, TOF-SIMS can be used to simultaneously provide both chemical information and distribution of various molecules in the sample surface down to the subcellular scale. Data obtained from this analysis of isotopes in the cell samples were used to calculate the relative amounts of long-chain PUFAs and phospholipids from their precursors, α-linolenic acid and linoleic acid. Our results show that the FA treatments induced an increase in the amounts of α-linolenic acid and linoleic acid and their long-chain conversion products.[JLR] Moreover, an enhanced level of phospholipid turnover of these FAs in lipids such as phosphatidylcholines, phosphatidylethanolamines, and phosphatidylinositols was also observed in the cell plasma membrane.—Philipsen, M. H., S. Sämfors, P. Malmberg, and A. G. Ewing. **Relative quantification of deuterated omega-3 and -6 FAs and their lipid turnover in PC12 cell membranes using TOF-SIMS.** *J. Lipid Res.* 2018. **59:** 2098–2107.

Supplementary key words time-of-flight secondary ion mass spectrometry • phospholipids • α-linolenic acid • linoleic acid • lipid turnover • fatty acids

The human body can synthesize all FAs it requires except for two, α-linolenic acid (ALA; 18:3n-3), which belongs to the omega-3 (n-3) family, and linoleic acid (LA; 18:2n-6), which belongs to the omega-6 (n-6) family. The FAs function as precursors for a series of n-3 and n-6 long-chain PUFAs via an FA synthesis process of desaturation and elongation reactions (1). PUFAs have been shown to exhibit health benefits in various ways and are involved in immune, heart, and brain function in addition to infant cognitive development (2). For example, ALA is converted into its metabolites, such as EPA (C20:5n-3) and DHA (C22:6n-3), which are important in immune regulation, inflammatory processes, and cognition (3). In addition, arachidonic acid (AA; C20:4n-6), a lipid that is partly converted from LA, is a key mediator and regulator of inflammation (4). The lack of intake of these two PUFAs increases the risk of diseases involving inflammatory processes such as obesity, cancer, and cardiovascular disease, as well as neurodegenerative illness (5, 6). Lower levels of DHA, EPA, and AA in human blood have also been shown to correlate with attention-deficit hyperactivity disorder and autism (7).

Changes in PUFAs after ALA and LA supplementation have been shown in preliminary studies to be useful in preventive treatment against neurodegenerative disease as well as cardiovascular disease (8–10). For example, n-3 PUFAs have been shown to be associated with the prevention and treatment of dementia and attention-deficit hyperactivity disorder (9, 11). Treatment with n-3 PUFA supplements that increase the n-3:n-6 PUFA ratio have been shown to reduce cognitive impairment in transgenic mice (12–14). The formation of new membranes induced by n-3 and n-6 FAs can influence the expansion of synaptic connections, which in turn can play an important role in neurotransmission (15, 16). Because the many roles of

---

PUFAs in biological processes are starting to be revealed, a proper understanding of their converted acid and phospholipid turnover is needed. This is especially true regarding the contribution of PUFAs and their specific phospholipid turnover in the prevention of age-related disruption of brain function. Several studies have revealed changes in lipids containing long-chain PUFAs after treatment with n-3 and n-6 FAs in rats and cells (17). However, the information about which specific phospholipids incorporate the FAs remains unknown. An understanding about membrane lipid turnover and the incorporation of PUFAs might provide a link between incorporation-specific lipids and mental illnesses.

Conventional MS approaches can be used to identify levels of FAs and lipids in biological samples (18). MS quantifies lipids with a low detection limit, high sensitivity, and wide dynamic range and provides a tool that combines quantitative and qualitative information with spatial localization of molecules on the sample surface. The material on the surface is removed by either a laser or ion beam and is then analyzed. In contrast to conventional approaches, the cell or tissue samples are directly analyzed without a requirement for further sample preparation (19). In recent years, time-of-flight secondary ion mass spectrometry (TOF-SIMS) has become widely used for MS imaging. It is applied in a wide range of application fields, such as materials, clinical research, and biomedical analysis, and uses a variety of different ion beams (Bi_n, C_{60}^+, Au_n) (19–21). Recently, the application of gas cluster ion beams (GCIBs) has shown great promise for the analysis of lipids. GCIBs have shown signal improvement for the analysis of intact lipid species with advantages that include low surface damage and reduced fragmentation (22, 23).

In this article, we took advantage of two types of TOF-SIMS instruments to obtain the chemical localization of biomolecules in cells: an IONTOF V equipped with a 25 keV bismuth liquid-metal ion gun (LMIG) and a J105 TOF-SIMS equipped with a 40 keV CO_2 GCIB. The detection of deuterated species at the nanoscale with high spatial resolution was carried out with the LMIG, whereas the GCIB provided higher signals for higher-mass species, such as intact lipids. The ability to combine good spatial resolution and high-mass molecular ion analysis provides more distribution-specific information of incorporated lipid species from n-3 and n-6 FAs on the cellular scale. We used stable isotopically labeled FAs to trace phospholipid synthesis and transport into the plasma membrane of pheochromocytoma cells (PC12) with TOF-SIMS. Deuterated and nondeuterated FAs were used to incubate cells, and then the relative amount of phospholipid turnover from FAs in the cellular membrane was determined based on the signals from the isotope peaks obtained from the TOF-SIMS spectra. Our data showed an increase in the content of FAs and phospholipids in the plasma membrane. Isotope substrate studies also indicated the incorporation of deuterated FAs into unsaturated phosphatidylcholines (PCs), phosphatidylethanolamines (PEs), and phosphatidylinisitols (PIs). From this we show that the conversion PUFAs from both

ALA and LA is different, and we suggest a pathway for lipids in the protection against unhealthy brain aging.

MATERIALS AND METHODS

Chemicals

[D5]ALA ($^2H_5C_{18}H_{25}O_2$; 283.25 g/mol) and [D2]LA ($^2H_2C_{18}H_{30}O_2$; 282.25 g/mol) were purchased from Lipidox (Stockholm, Sweden). [D2]LA was used in this study because of its accessibility. Nondeuterated ALA (18:3n-3; $C_{18}H_{30}O_2$; 278.22 g/mol) and LA (18:2n-6; $C_{18}H_{30}O_2$; 280.24 g/mol) were obtained from Sigma-Aldrich (Germany).

Cell sample preparation

The PC12 cell line was chosen to study the effects of PUFAs on the cell membrane because it has been characterized for studying neuronal functions and differentiation (24). PC12 cells were donated by Lloyd Greene (Columbia University). The cells were maintained in RPMI-1640 media (PAA Laboratories, Inc., Australia) supplemented with 10% donor equine serum (PAA Laboratories, Inc.) and 5% fetal bovine serum (PAA Laboratories, Inc.). The cells were plated in collagen-coated flasks (collagen type IV; BD Biosciences, Bedford, MA) and incubated in a 7% CO_2 100% humidity environment at 37°C. The cell medium was changed every 2 days, and the cells were subcultured every 7 days.

For experiments, cells were grown on poly-L-lysine-coated silicon wafers for 3 days. Cells were incubated with RPMI-1640 media supplemented with 10% donor equine serum and 5% fetal bovine serum (24) containing 100 μM deuterated or nondeuterated FAs (ALA and LA) for 1 day. ALA and LA were dissolved in ethanol and added to the medium to a final concentration of 0.1% ethanol before use. The silicon wafers were then rinsed three times with 50 mM ammonium formate (pH 7.4; Sigma-Aldrich). After removing the excess liquid on the surface, the silicon wafers were fast-frozen in isopentane at −185°C to avoid the formation of water crystals on the sample surface and thereafter freeze-dried. The samples were introduced into the analysis chamber of the TOF-SIMS instruments for analysis. Two silicon wafer slides containing cells for each sample were prepared. The experiments were repeated with three cell generations. Each generation was repeated twice.

TOF-SIMS imaging: IONTOF V

TOF-SIMS was performed with an IONTOF V (IONTOF GmbH, Münster, Germany) equipped with a 25 keV bismuth LMIG. The bunched mode with Bi_3^{2+} primary ions gave a high-mass resolution of 7,000 with a pulsed current of 0.3 pA. The primary ion dose density was 2×10^{12} ions/cm^2 in both positive and negative ion modes for an image area of 255 × 255 μm^2 with 256 × 256 pixels. A low-energy electron flood gun was used to neutralize the charge on the sample surface.

TOF-SIMS analysis: J105

TOF-SIMS analysis was also performed using a J105 TOF-SIMS instrument (Ionoptika Ltd., Eastleigh, UK) that has been described in detail elsewhere (25, 26). The instrument was equipped with a quasi-continuous primary ion beam that was used to bombard the sample to produce a stream of secondary ions that were bunched to produce a tight packet of ions at the entrance of a reflectron TOF analyzer. In this study, a 40 keV GCIB was used. Clusters were formed by the expansion of CO_2 into a vacuum chamber and further ionized by electron impact. The GCIB improves the surface smoothness and minimizes subsurface chemical damage due to its low individual atomic interactions. A Wien filter was

used to select a cluster size range of $n=6,000$ (approximately $\pm 2,000$). Spectra were acquired over an $800 \times 800 \ \mu m^2$ area at a pixel resolution of $6.26 \ \mu m^2$/pixel. The primary ion dose density for each image was approximately 1×10^{13} ions/cm^2. In the negative ion mode, low-energy (12 eV) electron flooding was used to decrease the effects from sample charging. The instrument provided a mass resolution of 10,000 for m/z 772.6.

Data analysis

TOF-SIMS spectra and images obtained from the IONTOF V were processed with Surface Lab version 6.3 (IONTOF GmbH). The region of interest covered only cells and was selected to minimize the contribution from background signals around the cells. The spectra obtained were calibrated to the peaks at CH_3^+, $C_2H_5^+$, $C_3H_7^+$, and the phosphocholine head-group fragment (27) $C_5H_{15}PNO_4^+$ for the positive ion mode and CH^-, C_2^-, C_3^-, and $C_{18}H_{33}O_2^-$ for the negative ion mode.

TOF-SIMS data from the J105 were processed using the Ionoptika Image Analyzer 2D program. Pixels containing cells were picked by imaging m/z 184.1 (PC fragment) for the positive ion mode and m/z 885.6 (PI 38:4) for the negative ion mode. Data were normalized to the number of pixels chosen in the region of interest. For the positive ion mode, data were normalized to the PC head group at m/z 184.1; for the negative ion mode, data were normalized to the PI head group at m/z 241.0. Spectra from the analysis after nonlabeled FA incubation were overlaid with spectra from the deuterium-labeled FA incubation and with a control sample in which no FAs were added to determine into which phospholipids the [D5]ALA and [D2]LA were incorporated.

Calculating the relative quantification of lipid species

To calculate the relative level of phospholipids incorporated into PC12 cell membranes, selected ions were normalized to the number of pixels per area of interest covered by the cells to subtract background signals. The signal intensities of PC species were then normalized to the peak at m/z 184.1 in the positive ion mode, whereas in the negative ion mode, intensities of the FA, PE, and PI species were normalized to the peak at m/z 241.0. This was performed on data from samples incubated with FAs (nonlabeled and deuterium-labeled FAs) as well as data from control samples (without the addition of exogenous FAs). Because of the peak overlap in the sample exposed with FA, the normalized peak intensity in FA samples was then subtracted from control peaks at the same m/z values to remove any interference. The relative amount of deuterated and nondeuterated phospholipids incorporated into the plasma membrane compared with control samples was calculated based on equation 1:

$$\text{Relative amount} = \frac{I_{\text{normalized-FA}} - I_{\text{normalized-control}}}{I_{\text{normalized-control}}} \quad \textit{(Eq. 1)}$$

where $I_{\text{normalized-FA}}$ is the normalized peak intensity at m/z +5 for [D5]ALA and m/z +2 for [D2]LA treatment and $I_{\text{normalized-control}}$ is the normalized peak intensity in the control at corresponding m/z values with FA incubation.

RESULTS

Uptake of deuterated n-3 ALA and n-6 LA into the plasma membrane

PC12 cells were incubated with deuterated and nondeuterated ALA and LA to determine the accumulation of FAs into the cell membrane. The advantage of using deuterium-labeled FAs is the ability to determine the FA accumulation and incorporation into longer-chain FAs, as well as the relative amount of phospholipids that incorporate into the cell membrane. The images of single cells collected with the IONTOF V demonstrate the localization of n-3 ALA and n-6 LA absorbed into the cell membrane. The mass spectra of FA species are also provided in supplemental Figure S1.

Figure 1 shows the negative ion TOF-SIMS images of the control and incubated samples. The intensity of the peak at m/z 277.2 was more dominant compared with the same peak in the control and [D5]ALA samples (Fig. 1A–C). The cells treated with [D5]ALA revealed a high-intensity peak at m/z 282.3, whereas the same peak in the control cells or those incubated with nondeuterated ALA was low (Fig. 1D–F). Similarly, we observed LA incorporation in the sample incubated with LA and [D2]LA. Figure 1H exhibits the more dominant FA (18:2) at the m/z 279.2 peak for LA. In contrast, in the sample incubated with [D2]LA, a more intense peak at m/z 281.2 was observed compared with the other samples (Fig. 1L). We also observed that the abundance of FA 18:1 at m/z 281.2 in the sample with LA treatment was higher compared with the control. This was caused by an overlap between FA 18:1 and [D2]FA 18:2 with the same peak at m/z 281.2.

n-3 ALA and n-6 LA synthesis in the plasma membrane

In the sample incubated with [D5]ALA, the ion species with m/z +5 represented the incorporation of phospholipids and did not overlap with any endogenous fragments in the mass spectrum. However, most of the molecules with m/z +2 selected in the sample treated with [D2]LA overlapped with other endogenous phospholipids. To confirm that the signal change after incubation was indeed from the converted FAs from [D2]LA, the spectrum from the nondeuterated LA treatment was also examined. The peak for the nondeuterated FA was compared with the peak two mass units higher (m/z +2) for the deuterated sample. **Table 1** gives assignments for the peaks incubated with labeled and nonlabeled ALA and LA. All peaks analyzed, in nondeuterated and deuterated forms, are provided in supplemental Tables S1 and S2.

After incubation with ALA, the spectra obtained from the TOF-SIMS J105 analysis in the negative ion mode (**Fig. 2A**) showed increases in FAs with 20 and 22 carbons for both the n-3 ALA and [D5]ALA. The peaks at m/z 301.2, 303.2, 305.2, 329.3, 331.3, and 333.3 were the [M-H]$^-$ ions of FAs 20:5, 20:4, 20:3, 22:5, 22:4, and 22:3, respectively, and were shown to increase in the spectrum from the samples incubated with nonlabeled ALA.

For the incubation with the [D5]ALA, an increase in the same FA peaks was observed at five mass units higher due to the five deuterium labels; hence, the peaks at m/z 306.2, 308.2, 310.2, 334.3, 336.3, and 338.3 can be observed to increase (Fig. 2A). This observed change of the [D5]ALA indicates that the increase was due to conversion to the FAs followed by incorporation of the incubated ALA into the cell membrane and not an upregulation of endogenous FAs. The well-established metabolic pathway for C18:3n-3
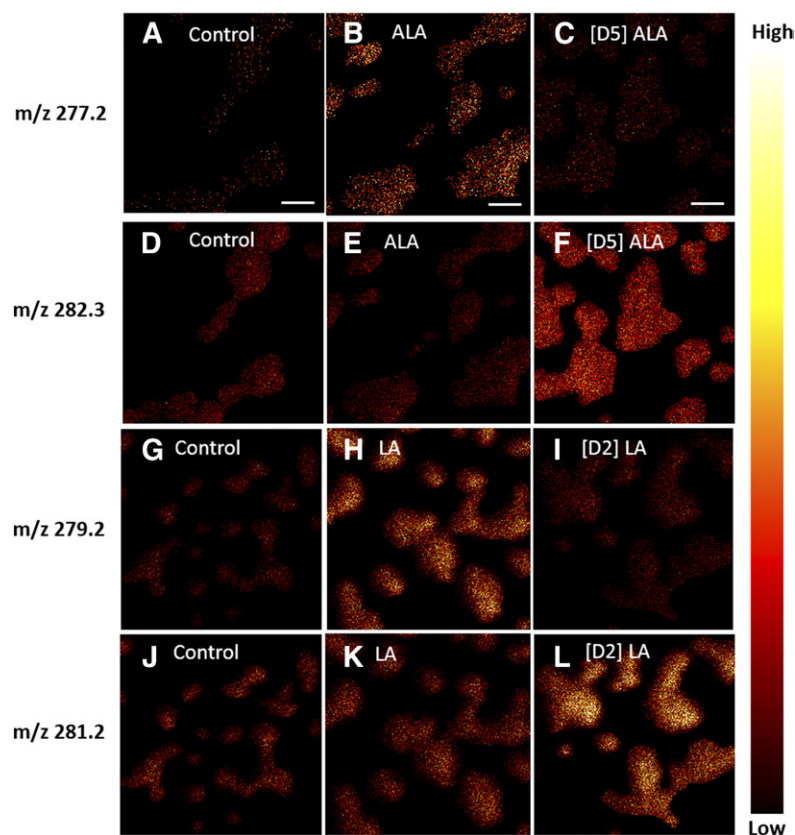
Fig. 1. TOF-SIMS ion images showing the accumulation of FAs into the cell membrane using the IONTOF V equipped with a 25 keV Bi$_3^{2+}$ LMIG in the negative ion mode. A–C: Control, ALA-treated cells, and [D5] ALA-treated cells at *m/z* 277.2, respectively. D–F: Control, ALA-treated cells, and [D5]ALA-treated cells at *m/z* 282.3, respectively. G–I: Control, LA-treated cells, and [D2]LA-treated cells at *m/z* 279.2, respectively. J–L: Control, LA-incubated cells, and [D2]LA-incubated cells at *m/z* 281.2, respectively. Image area: 255 × 255 μm^2 and 256 × 256 pixels. Scale bar = 40 μm.

ALA in biological systems gives rise to longer-chain PUFAs such as C20:4, C20:5, C22:5, and C22:6 in a series of steps. This corresponds well with the observed increase in FAs shown in Fig. 2A. However, there was no change observed in FA 22:6 in our experiments using TOF-SIMS. The FA 22:6 is the end product in the FA synthesis pathway. Thus, the amount of FA 22:6 created from the conversion of the incubated ALA is apparently too small to be able to observe any significant differences between the control and ALA-incubated samples (28).

The same trends are observed in Fig. 2B for the incubation with LA C18:2n-6, where LA was readily converted into longer-chain PUFAs, including FAs 20:4, 20:3, 20:2, and 20:1. The increase in these PUFAs was detected for both incubation with nonlabeled LA and [D2]LA, the same observation as for the ALA-incubated samples. However, there was no significant increase in the long-chain conversion of FAs with 22 carbons. Our finding is consistent with the synthesis pathway of n-6 LA in human and animal models, where LA is mostly converted into low long-chain FAs with 20 carbons (1, 29, 30). The observed increase in specific FAs for the LA and [D2]LA incubation matches well with the metabolic pathway for LA in biological systems, where it is converted to C18:3, C20:3, C20:4, C22:4, and C22:5.

Incorporation of ALA and LA into plasma phospholipids

PC12 cells internalize the supplemental n-3 and n-6 FAs and proceed to the metabolic conversion and incorporation

TABLE 1. Assignment for selected peaks for samples incubated with deuterated and nondeuterated ALA and LA

|	Nondeuterated ALA		[D5]ALA		Nondeuterated LA		[D2]LA	
	Measured *m/z*	Assignment	Measured *m/z*	Assignment	Measured *m/z*	Assignment	Measured *m/z*	Assignment
Positive ion mode [M+H]$^+$	760.6	PC 34:1	765.6	[D5]PC 34:1	758.6	PC 34:2	760.6	[D2]PC 34:2
	794.5	PC 34:3 + K	799.5	[D5]PC 34:3 + K	786.6	PC 36:2	788.6	[D2]PC 36:2
	806.6	PC 38:6	811.6	[D5]PC 38:6	808.6	PC 36:2 + Na	810.6	[D2]PC 36:2 + Na
	808.6	PC 38:5	813.6	[D5]PC 38:5	824.6	PC 36:2 + K	826.6	[D2]PC 36:2 + K
	818.5	PC 36:5 + K	823.5	[D5]PC 36:5 + K	852.6	PC 38:2 + K	854.6	[D2]PC 38:2 + K
	820.5	PC 36:4 + K	825.5	[D5]PC 36:4 + K				
	822.5	PC 36:3 + K	827.5	[D5]PC 36:3 + K				
Negative ion mode [M-H]$^-$	740.5	PE 36:3	745.5	[D5]PE 36:3	742.5	PE 36:2	744.5	[D2]PE 36:2
	764.5	PE 38:5	769.5	[D5]PE 38:5	770.6	PE 38:2	772.6	[D2]PE 38:2
	766.5	PE 38:4	771.5	[D5]PE 38:4	861.6	PI 36:2	863.6	[D2]PI 36:2
	768.6	PE 38:3	773.6	[D5]PE 38:3	885.6	PI 38:4	887.6	[D2]PI 38:4
	859.5	PI 36:3	864.5	[D5]PI 36:3				
	883.5	PI 38:5	888.5	[D5]PI 38:5				
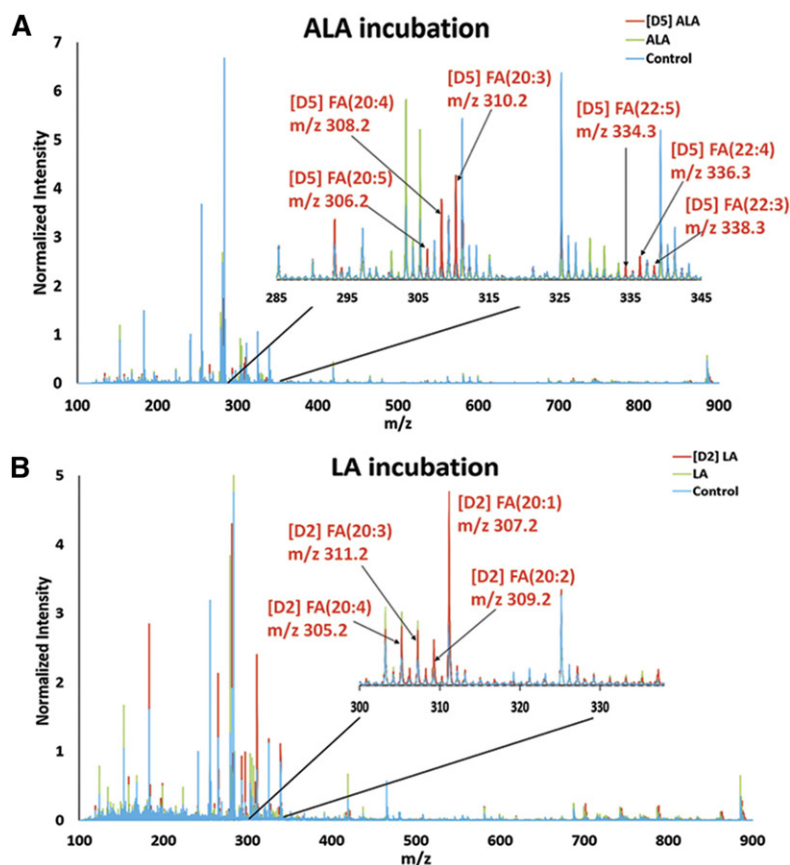
Fig. 2. Overlaid spectra of converted FAs from incubation with (A) ALA and [D5]ALA and (B) LA and [D2]LA analyzed using a J105/40 keV $(CO_2)_{6000}^+$ GCIB (negative ions). Peak intensity was normalized to the number of pixels selected and the PI fragment at m/z 241.0.

of the FAs into the phospholipids in the cell membrane (1). To identify the incorporation of the n-3 ALA and n-6 LA into the cell membrane, the mass spectra of control, deuterated, and nondeuterated samples were compared to track the deuterium labels on the FAs used for incubation. The ion dose was kept below the static limit to confirm that the analyzed species originates from the cell membrane and not from the cytoplasm. As mentioned above, the peaks at m/z +5 and m/z +2 in cells incubated with [D5]ALA and [D2] LA, respectively, were chosen and then confirmed with the nondeuterated forms of the same species.

Figure 3 shows the conversion and incorporation of ALA and [D5]ALA into phospholipids. For example, in the negative ion mode, we found that the peaks for PEs 36:3, 38:3, 38:4, and 38:5 and PIs 36:3 and 38:5 were increased in the spectra after incubation with ALA or the [D5]ALA, indicating an incorporation of ALA into this species (Fig. 3B).

Figure 4 reveals the incorporation of LA into phospholipids, where an increase can be seen for different species. For example, the signal intensities of PEs 36:2 and 38:2 and PIs 36:2 and 38:4 observed in the negative ion mode give a higher signal intensity in FA-incubated samples compared with the control (Fig. 4B). Table 1 provides a complete list of the phospholipid peaks that changed after incubation for both the ALA and LA incubation (with and without the deuterium label). In general, the synthesis of PCs, PEs, and PIs use ALA for incorporation into lipids with three, five, and six double bonds, whereas LA incorporates into phospholipids with two and four double bonds.

Comparison of the incorporation levels for ALA and LA into cellular phospholipids

The peaks at m/z 184.1 and 241.0 are head-group fragment ions of PC and PI, respectively, and we used these as the membrane standard. To calculate the level of incorporation, we assumed that the total amount of endogenous phospholipids stays unchanged. Therefore, the intensity of PC and PI head-group fragments was approximately similar or only slightly altered in all the samples. The change in the signal after both the nondeuterated LA and deuterated treatment was then used to establish the amount of phospholipid turnover. The level of incorporation was calculated for both treatments and compared with each other.

To identify the phospholipid turnover and their relative amounts, both nondeuterated and deuterated FAs were exposed to the cells. The nondeuterated FA incubation was used for comparison with the enrichment caused from deuterium-labeled FAs. The relative level of FA and phospholipid incorporation into the plasma membrane was calculated using the intensity ratio between the control and treated samples (equation 1).

As expected, an increased amount of ALA and LA was found in PC12 cell membranes in treated samples (supplemental Fig. S2). Interestingly, the accumulation of ALA was ~50% higher than LA in the cell membrane ($P<0.05$), even when their incubation concentrations in the experiments were the same. In the treated samples, the incorporation level of ALA increased 2-fold compared with a 150%
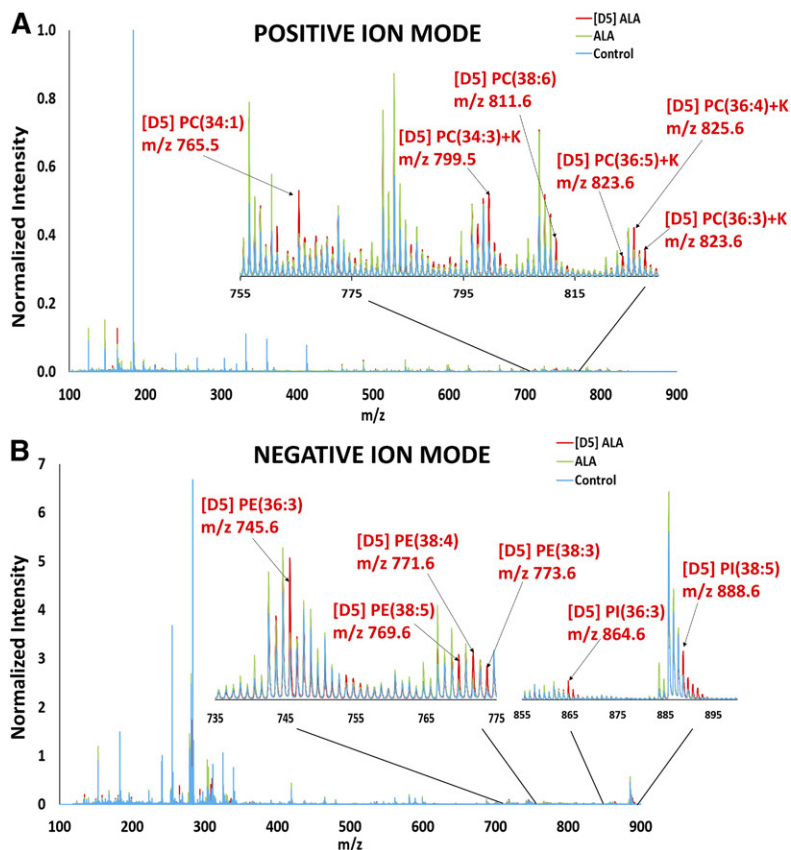
Fig. 3. Phospholipid turnover from ALA and [D5] ALA in (A) positive ion mode and (B) negative ion mode analyzed using a J105/40 keV $(CO_2)_{6000}^+$ GCIB. Peak intensity was normalized to the number of pixels selected and the PC fragment at m/z 184.1 (positive mode) or PI fragment at m/z 241.0 (negative mode). PCs were detected as [M+H]$^+$ ions unless specified as +K. PEs and PIs were detected as [M-H]$^-$.

increase for LA compared with the controls. We also obtained the relative amount of long-chain PUFAs converted from those FAs. Most of the FA species, such as FAs 20:5, 20:4, 20:3, 22:5, and 22:4, biosynthesized from ALA were 100% to 150% higher than the level observed in control cells. Our data are supported by Hussein et al. (31), who used [^{13}C]ALA and LA. They also found a >3-fold increase in ALA and 2-fold increase in FAs 20:5 and 22:5 in erythrocyte membranes in human blood samples when incubated with lipids (31). In contrast, a smaller increase in FA 22:3 (~50%) was found in the ALA-treated sample. Similarly, we obtained an increase in metabolites of LA in

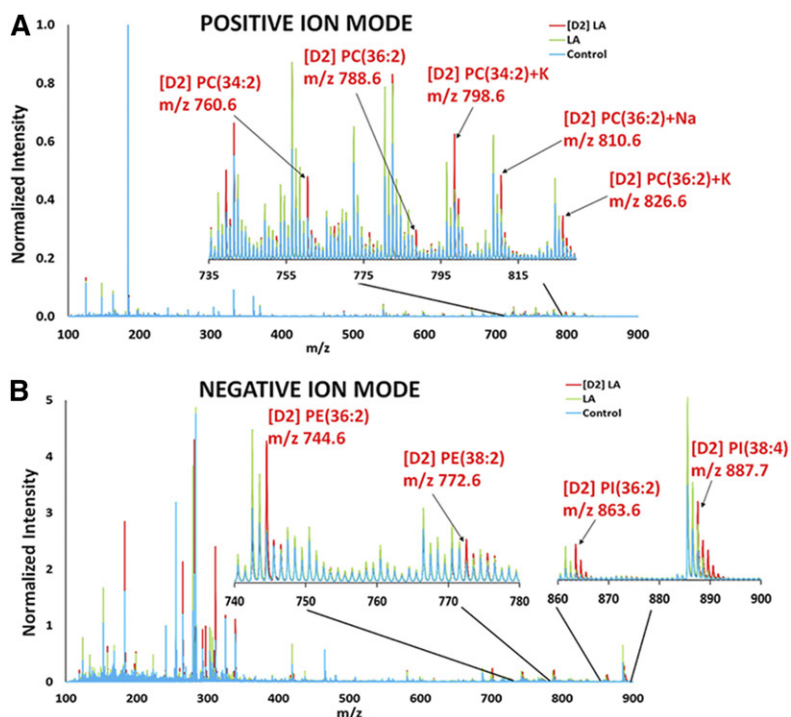**Fig. 4.** Phospholipid turnover from LA and [D2]LA in (A) positive ion mode and (B) negative ion mode analyzed using a J105/40 keV $(CO_2)_{6000}^+$ GCIB. Peak intensity was normalized to the number of pixels selected and the PC fragment at m/z 184.1 (positive mode) or PI fragment at m/z 241.0 (negative mode). PCs were detected as [M+H]$^+$ ions unless specified as +K or +Na. PEs and PIs were detected as [M-H]$^-$.
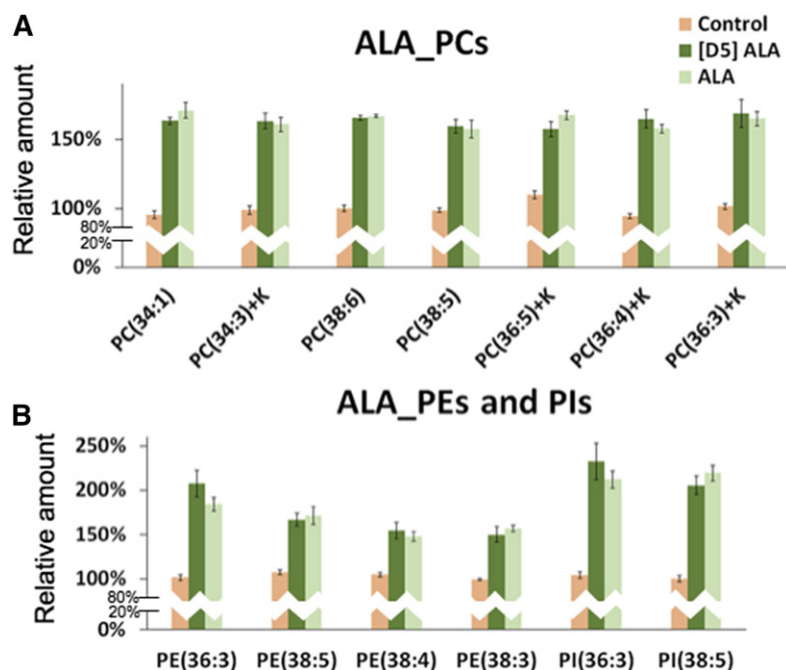
Fig. 5. The relative amount of phospholipids after incubation with ALA and [D5]ALA for (A) PC molecules in the positive ion mode and (B) PE and PI species in the negative ion mode analyzed using a J105/40 keV $(CO_2)_{6000}^+$ GCIB. The increase was calculated by comparing to the control samples. Peak intensity was normalized to the number of pixels selected and the PC head group at m/z 184.1 for the positive ion mode or the PI fragment at m/z 241.0 for the negative ion mode. The error bars show the SEMs. The relative levels of phospholipids were calculated for three cell generations.

the LA-exposed sample. For example, FAs 20:4 and 20:1 increased approximately 50%, whereas FAs 20:3 and 20:2 approximately doubled compared with the control.

Figure 5 shows the increase in the relative amount of phospholipids after incubation with ALA and [D5]ALA compared with the control ($\sim$100%; supplemental Table S3). In the positive ion mode, the amount of PC turnover increased by $\sim$60%. Likewise, PE species in treated samples, such as PEs 38:5, 38:4, and 38:3, were found to be 50% to 70% higher compared with the control, except PE 36:3, which was $\sim$90% higher. However, the amount of PE turnover was about half the level of incorporated PI in ALA-treated samples. For example, a 110% increase in PIs 36:3 and 38:5 was found. Consistent with our results, others have shown similar amounts of incorporation of ALA and its converted PUFAs into PCs and PEs in human Y79 retinoblastoma cells (32).

The comparison between the relative amount of phospholipid turnover from LA and [D2]LA was examined to confirm the actual amount of incorporated phospholipids into cell membranes and to rule out incorporation from other endogenous lipids. **Figure 6** shows the increase in the relative amount of phospholipids after incubation with LA and [D2]LA compared with the control ($\sim$100%; supplemental Table S4). Cells incubated with LA had a phospholipid turnover that was significantly increased compared with nontreated control cells. The amount of PCs synthesized by LA and its converted PUFAs were approximately 40% to 50% higher than nontreated samples. Almost 100% of PE and PI levels, especially PE 36:2 and PI 36:2, were increased in LA-incubated cells, whereas an increase of $\sim$60% in PE 38:2 and PI 38:4 was observed. Overall, the amount of total phospholipids incorporated from LA was $\sim$40% less than those from ALA, although the same concentrations of ALA and LA were used for incubation ($P <$ 0.05). This finding was correlated with the amount of FAs

incorporated in the cell membrane and is shown in supplemental Fig. S2.

DISCUSSION

Understanding lipid metabolism is important in gaining more knowledge about cell functions. Therefore, using stable isotopic-labeled substrates, we were able to track the incorporation of the essential FAs into other FA products as well as the incorporation into phospholipids. The stable isotopic-labeled substrates also make it possible to determine the relative quantitative information of incorporated products in the plasma membrane, providing new insights into membrane lipid metabolism. Here, we introduced a method for visualizing and relatively quantifying phospholipids in the PC12 cell membrane. TOF-SIMS analysis with two instruments, one using an LMIG and another a GCIB, provided spatial information about the incorporated FAs as well as the ability to detect intact lipid species.

The n-3 and n-6 FAs cannot be synthesized by the cell and therefore need to be provided by an exogenous (dietary) source. The accumulation of both n-3 and n-6 FAs in cellular membranes and tissues has been shown in previous studies (33, 34), indicating that the essential FAs are of particular importance in maintaining critical functions for the cell and are therefore important for the cell to store in the form of various phospholipids in, for example, cellular membranes. In this experiment, TOF-SIMS showed that the increased level of ALA and LA observed after incubation suggests a high uptake of both the FAs into the cell from the surrounding media. In addition, the results from incubation with deuterium-labeled FAs revealed that the formation of converted PUFAs from ALA and LA are different. Only PUFAs with 20 carbons were produced from LA, whereas ALA could convert into PUFAs with both
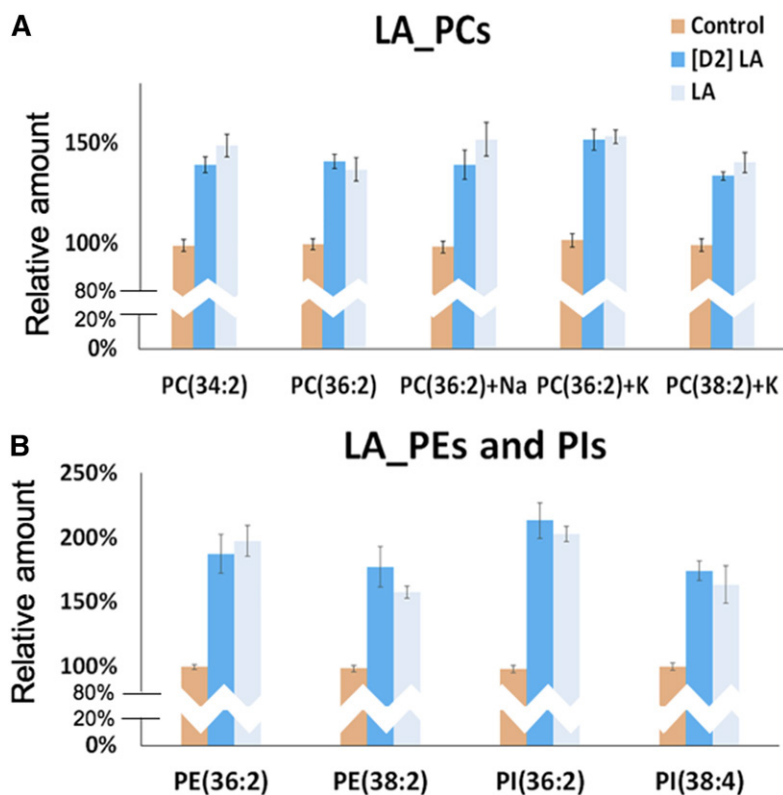
A LA_PCs

Legend: Control, [D2] LA, LA

B LA_PEs and PIs

Fig. 6. The relative amount of phospholipids after incubation with LA and [D2]LA for (A) PC species in the positive ion mode and (B) PE and PI species in the negative ion mode analyzed using a J105/40 keV $(CO_2)_{6000}^+$ GCIB. The increase was calculated by comparing to the control samples. Peak intensity was normalized to the number of pixels selected and the PC head group at m/z 184.1 for the positive ion mode or the PI fragment at m/z 241.0 for the negative ion mode. The error bars show the SEMs. The relative levels of phospholipids were calculated for three cell generations.

20 and 22 carbons. In addition, our data suggest that ALA (with three double bonds) or its conversion product EPA C20:5 (with five double bonds) is incorporated without the further addition of double bonds in either one or both FA positions in the phospholipid, creating lipid molecules with three, five, or six double bonds. The same is true for LA (with two double bonds) and the conversion product AA (with four double bonds), which might be incorporated into phospholipids to create lipids with two and four double bonds.

It is important to note that the various unsaturated phospholipids that were generated originated from ALA and LA in the cell membrane. The data further indicate that the ALA and LA are converted and incorporated into a range of lipid species such as PC, PE, and PI (see Figs. 3 and 4, Table 1). The selectivity of incorporation of PUFAs into phospholipids has been previously investigated, where incorporation into PC and PE was found (35, 36). It has also been shown that ALA is converted to DHA in the developing rat brain (37) and can thereafter be incorporated into specific phospholipids such as PC, PE, and PI in vivo (38). The same is true in studies of cells. For example, Li et al. (39) and Stulnig et al. (40) reported that T cells incubated with EPA 20:5n-3, which is part of the metabolic pathway for ALA, shows altered lipid membrane composition, where enrichment is observed in the PE species substituted with 36:5, 38:6, 38:5, 40:7, 40:6, and 40:5 acyl chains, PI species substituted with 36:4, 38:5, 40:6, and 40:5 acyl chains, and PC species substituted with 36:3, 36:4, 38:6, 38:5 and 40:6 acyl chains. The results from these previous studies are in good agreement with the differences in cell membrane composition observed between the control cells

and the ALA- or LA-incubated cells, where these are incorporated into PC, PE, and PI.

Based on TOF-SIMS data, the relative amounts of phospholipid turnover generated from ALA and LA in the plasma membrane was calculated using the intensity ratio between the control and treated samples. We found that the accumulated amount of ALA and its converted PUFAs was more than that of LA and its long-chain PUFAs. From those results, we suggest that the relative levels of phospholipids synthesized by LA is less than by ALA. This is an important finding because unsaturated phospholipids incorporated into the cell membrane can alter the physical properties of the membrane, such as flexibility and solubility, which promotes the membrane fluidity. Moreover, the flexible unsaturated PUFAs also stimulate the formation of the SNARE complex in vesicle fusion that plays an important role in exocytosis (41). It is well known that the consumption of n-3 and n-6 FAs can change the plasma membrane lipid compositions, which in turn can reduce the risk of mental disorders (42). Of course, these experiments were all done in a relatively high-concentration format compared with tracer experiments to facilitate detection. These higher concentrations might lead to a small perturbation in the system. In defense of this approach, we previously found that 100 μM lipid incubations of PC12 cells result in an ∼1% change in lipid in the cell membrane (43).

CONCLUSIONS

We used TOF-SIMS to image and analyze lipids in PC12 cell membranes with and without treatment with n-3 and -6 FAs and simultaneously measured both the chemistry and

distribution of various lipids in the cell membrane. We then analyzed the different isotopes in cell samples to calculate the relative amounts of long-chain PUFAs and phospholipids compared with their precursors, ALA and LA. Treatment with the n-3 and -6 FAs induced an increase in the amount of ALA and LA and their long-chain conversion products. The turnover of these FAs in the overall phospholipids, especially phosphatidylcholines, phosphatidylethanolamines, and phosphatidylinositols, was also observed in the cell plasma membrane. Our findings are important for understanding which specific phospholipids might be involved in the neurodegenerative diseases and suggest a basic pathway for protection against unhealthy brain aging.

REFERENCES

1. Emken, E. A., R. O. Adlof, H. Rakoff, W. K. Rohwedder, and R. M. Gulley. 1990. Metabolism in vivo of deuterium-labelled linolenic and linoleic acids in humans. *Biochem. Soc. Trans.* **18:** 766–769.

2. Wall, R., R. P. Ross, G. F. Fitzgerald, and C. Stanton. 2010. Fatty acids from fish: the anti-inflammatory potential of long-chain omega-3 fatty acids. *Nutr. Rev.* **68:** 280–289.

3. Weiser, M. J., C. M. Butt, and M. H. Mohajeri. 2016. Docosahexaenoic acid and cognition throughout the lifespan. *Nutrients.* **8:** 99.

4. Calder, P. C. 2009. Polyunsaturated fatty acids and inflammatory processes: new twists in an old tale. *Biochimie.* **91:** 791–795.

5. Corsinovi, L., F. Biasi, G. Poli, G. Leonarduzzi, and G. Isaia. 2011. Dietary lipids and their oxidized products in Alzheimer's disease. *Mol. Nutr. Food Res.* **55 (Suppl. 2):** S161–S172.

6. Khandelwal, S., L. Kelly, R. Malik, D. Prabhakaran, and S. Reddy. 2013. Impact of omega-6 fatty acids on cardiovascular outcomes: a review. *J. Preventive Cardiol.* **2:** 325–336.

7. Parletta, N., T. Niyonsenga, and J. Duff. 2016. Omega-3 and omega-6 polyunsaturated fatty acid levels and correlations with symptoms in children with attention deficit hyperactivity disorder, autistic spectrum disorder and typically developing controls. *PLoS One.* **11:** e0156432.

8. Kidd, P. M. 2007. Omega-3 DHA and EPA for cognition, behavior, and mood: clinical findings and structural-functional synergies with cell membrane phospholipids. *Altern. Med. Rev.* **12:** 207–227.

9. Schaefer, E. J., V. Bongard, A. S. Beiser, S. Lamon-Fava, S. J. Robins, R. Au, K. L. Tucker, D. J. Kyle, P. W. Wilson, and P. A. Wolf. 2006. Plasma phosphatidylcholine docosahexaenoic acid content and risk of dementia and Alzheimer disease: the Framingham Heart Study. *Arch. Neurol.* **63:** 1545–1550.

10. Jump, D. B., C. M. Depner, and S. Tripathy. 2012. Omega-3 fatty acid supplementation and cardiovascular disease. *J. Lipid Res.* **53:** 2525–2545.

11. Bos, D. J., B. Oranje, E. S. Veerhoek, R. M. Van Diepen, J. M. Weusten, H. Demmelmair, B. Koletzko, M. G. de Sain-van der Velden, A. Eilander, M. Hoeksma, et al. 2015. Reduced symptoms of inattention after dietary omega-3 fatty acid supplementation in boys with and without attention deficit/hyperactivity disorder. *Neuropsychopharmacology.* **40:** 2298–2306.

12. Delpech, J. C., C. Madore, C. Joffre, A. Aubert, J. X. Kang, A. Nadjar, and S. Laye. 2015. Transgenic increase in n-3/n-6 fatty acid ratio protects against cognitive deficits induced by an immune challenge through decrease of neuroinflammation. *Neuropsychopharmacology.* **40:** 525–536.

13. Molfino, A., G. Gioia, F. Rossi Fanelli, and M. Muscaritoli. 2014. The role for dietary omega-3 fatty acids supplementation in older adults. *Nutrients.* **6:** 4058–4073.

14. Dangour, A. D., V. A. Andreeva, E. Sydenham, and R. Uauy. 2012. Omega 3 fatty acids and cognitive health in older people. *Br. J. Nutr.* **107 (Suppl. 2):** S152–S158.

15. Marszalek, J. R., C. Kitidis, A. Dararutana, and H. F. Lodish. 2004. Acyl-CoA synthetase 2 overexpression enhances fatty acid internalization and neurite outgrowth. *J. Biol. Chem.* **279:** 23882–23891.

16. Darios, F., and B. Davletov. 2006. Omega-3 and omega-6 fatty acids stimulate cell membrane expansion by acting on syntaxin 3. *Nature.* **440:** 813–817.

17. Ikeda, I., K. Mitsui, and K. Imaizumi. 1996. Effect of dietary linoleic, alpha-linolenic and arachidonic acids on lipid metabolism, tissue fatty acid composition and eicosanoid production in rats. *J. Nutr. Sci. Vitaminol. (Tokyo).* **42:** 541–551.

18. Hoene, M., J. Li, H. U. Haring, C. Weigert, G. Xu, and R. Lehmann. 2014. The lipid profile of brown adipose tissue is sex-specific in mice. *Biochim. Biophys. Acta.* **1842:** 1563–1570.

19. Malmberg, P., E. Jennische, D. Nilsson, and H. Nygren. 2011. High-resolution, imaging TOF-SIMS: novel applications in medical research. *Anal. Bioanal. Chem.* **399:** 2711–2718.

20. Cheng, J., J. Kozole, R. Hengstebeck, and N. Winograd. 2007. Direct comparison of Au_3^+ and C_{60}^+ cluster projectiles in SIMS molecular depth profiling. *J. Am. Soc. Mass Spectrom.* **18:** 406–412.

21. Richter, K., H. Nygren, P. Malmberg, and B. Hagenhoff. 2007. Localization of fatty acids with selective chain length by imaging time-of-flight secondary ion mass spectrometry. *Microsc. Res. Tech.* **70:** 640–647.

22. Angerer, T. B., P. Blenkinsopp, and J. S. Fletcher. 2015. High energy gas cluster ions for organic and biological analysis by time-of-flight secondary ion mass spectrometry. *Int. J. Mass Spectrom.* **377:** 591–598.

23. Fletcher, J. S., S. Rabbani, A. M. Barber, N. P. Lockyer, and J. C. Vickerman. 2013. Comparison of C-60 and GCIB primary ion beams for the analysis of cancer cells and tumour sections. *Surf. Interface Anal.* **45:** 273–276.

24. Greene, L. A., and A. S. Tischler. 1976. Establishment of a noradrenergic clonal line of rat adrenal pheochromocytoma cells which respond to nerve growth factor. *Proc. Natl. Acad. Sci. USA.* **73:** 2424–2428.

25. Fletcher, J. S., S. Rabbani, A. Henderson, P. Blenkinsopp, S. P. Thompson, N. P. Lockyer, and J. C. Vickerman. 2008. A new dynamic in mass spectral imaging of single biological cells. *Anal. Chem.* **80:** 9058–9064.

26. Hill, R., P. Blenkinsopp, S. Thompson, J. Vickerman, and J. S. Fletcher. 2011. A new time-of-flight SIMS instrument for 3D imaging and analysis. *Surf. Interface Anal.* **43:** 506–509.

27. Phan, N. T. N., M. Munem, A. G. Ewing, and J. S. Fletcher. 2017. MS/MS analysis and imaging of lipids across Drosophila brain using secondary ion mass spectrometry. *Anal. Bioanal. Chem.* **409:** 3923–3932.

28. Pawlosky, R. J., J. R. Hibbeln, J. A. Novotny, and N. Salem, Jr. 2001. Physiological compartmental analysis of alpha-linolenic acid metabolism in adult humans. *J. Lipid Res.* **42:** 1257–1265.

29. Demmelmair, H., B. Iser, A. Rauh-Pfeiffer, and B. Koletzko. 1999. Comparison of bolus versus fractionated oral applications of [13C]-linoleic acid in humans. *Eur. J. Clin. Invest.* **29:** 603–609.

30. Su, H. M., T. N. Corso, P. W. Nathanielsz, and J. T. Brenna. 1999. Linoleic acid kinetics and conversion to arachidonic acid in the pregnant and fetal baboon. *J. Lipid Res.* **40:** 1304–1312.

31. Hussein, N., E. Ah-Sing, P. Wilkinson, C. Leach, B. A. Griffin, and D. J. Millward. 2005. Long-chain conversion of [13C]linoleic acid and alpha-linolenic acid in response to marked changes in their dietary intake in men. *J. Lipid Res.* **46:** 269–280.

32. Goustard-Langelier, B., J. M. Alessandri, G. Raguenez, G. Durand, and Y. Courtois. 2000. Phospholipid incorporation and metabolic conversion of n-3 polyunsaturated fatty acids in the Y79 retinoblastoma cell line. *J. Neurosci. Res.* **60:** 678–685.

33. Healy, D. A., F. Wallace, E. Miles, P. Calder, and P. Newsholme. 2000. Effect of low-to-moderate amounts of dietary fish oil on neutrophil lipid composition and function. *Lipids.* **35:** 763–768.

34. Bazan, N. G., and B. Scott. 1990. Dietary omega-3 fatty acids and accumulation of docosahexaenoic acid in rod photoreceptor cells of the retina and at synapses. *Ups. J. Med. Sci. Suppl.* **48:** 97–107.

35. Masui, H., R. Urade, and M. Kito. 1997. Selective incorporation of polyunsaturated fatty acids into organelle phospholipids of animal cells. *Biosci. Biotechnol. Biochem.* **61:** 900–902.

36. Lands, W. E., M. Inoue, Y. Sugiura, and H. Okuyama. 1982. Selective incorporation of polyunsaturated fatty acids into phosphatidylcholine by rat liver microsomes. *J. Biol. Chem.* **257:** 14968–14972.

37. Dhopeshwarkar, G. A., and C. Subramanian. 1976. Biosynthesis of polyunsaturated fatty acids in the developing brain: I. Metabolic

transformations of intracranially administered 1-14C linolenic acid. *Lipids.* **11:** 67–71.

38. Green, P., and E. Yavin. 1993. Elongation, desaturation, and esterification of essential fatty acids by fetal rat brain in vivo. *J. Lipid Res.* **34:** 2099–2107.

39. Li, Q., L. Tan, C. Wang, N. Li, Y. Li, G. Xu, and J. Li. 2006. Polyunsaturated eicosapentaenoic acid changes lipid composition in lipid rafts. *Eur. J. Nutr.* **45:** 144–151.

40. Stulnig, T. M., J. Huber, N. Leitinger, E-M. Imre, P. Angelisová, P. Nowotny, and W. Waldhäusl. 2001. Polyunsaturated eicosapentae-noic acid displaces proteins from membrane rafts by altering raft lipid composition. *J. Biol. Chem.* **276:** 37335–37340.

41. Darios, F., E. Connell, and B. Davletov. 2007. Phospholipases and fatty acid signalling in exocytosis. *J. Physiol.* **585:** 699–704.

42. Cole, G. M., Q. L. Ma, and S. A. Frautschy. 2010. Dietary fatty acids and the aging brain. *Nutr. Rev.* **68 (Suppl. 2):** S102–S111.

43. Lanekoff, I., P. Sjövall, and A. G. Ewing. 2011. Relative quantification of phospholipid accumulation in the PC12 cell plasma membrane following phospholipid incubation using TOF-SIMS imaging. *Anal. Chem.* **83:** 5337–5343.